Photorefractive self-focusing and defocusing as an optical limiter

Galen C. Duree Jr. and Gregory J. Salamo

University of Arkansas
Physics Department
Fayetteville, Arkansas 72701

Mordechai Segev and Amnon Yariv

California Institute of Technology
Department of Applied Phyiscs
Pasadena, California 91125

Edward J. Sharp

Army Research Laboratory
Fort Belvoir, Virginia 22060

and

Ratnakar R. Neurgankar

Rockwell International Science Center
Thousand Oaks, California 91360

ABSTRACT

Focusing and defocusing of laser light has been observed for many years. Optical Kerr type materials exhibit this effect only for high intensities. We show experimental evidence that photorefractive materials can also produce dramatic focusing and defocusing. Whereas Kerr materials produce this effect for high intensities, photorefractive materials produce these effects independent of intensity indicating that this effect would be ideal for an optical limiter. We compare the characteristics of Kerr and photorefractive materials, discuss the physical models for both materials and present experimental evidence for photorefractive defocusing. Self-focusing and defocusing was observed for any incident polarization although the effect was more pronounced using extraordinary polarized light. In addition, self-focusing or defocusing could be observed depending on the direction of the applied electric field. When the applied field was in the same direction as the crystal spontaneous polarization, focusing was observed. When the applied field was opposite the material spontaneous polarization, the incident laser light was dramatically defocused.

0-8194-1533-2/94/$6.00

INTRODUCTION

One of the attractive features of laser light is that it can be focused to a very small spot. While a small, intense laser spot has found many useful applications, it is this same feature which makes laser light dangerous to the eye and to optical sensors in general. One class of materials which has been proposed to limit the transmission of high intensity laser light are Kerr materials. Optical limiters based on the use of optical Kerr materials take advantage of the fact that these materials exhibit an intensity dependent refractive index given by

$$n = n_0 + n_2 I \tag{1}$$

where n_0 and n_2 are material constants. Since the incident laser beam usually has a near Gaussian intensity profile, the index of refraction of the material mimic the beam and possesses a Gaussian profile as well as shown in Figure 1. In this case n_2 is assumed positive. The result is that the laser beam itself induces a lensing effect which in this case focuses the laser beam in much the same way that a converging lens focuses a laser beam. If on the other hand the material chosen has a material constant n_2 which is negative then the laser beam would induce a defocusing effect and affect the beam in a manner similar to a diverging lens.

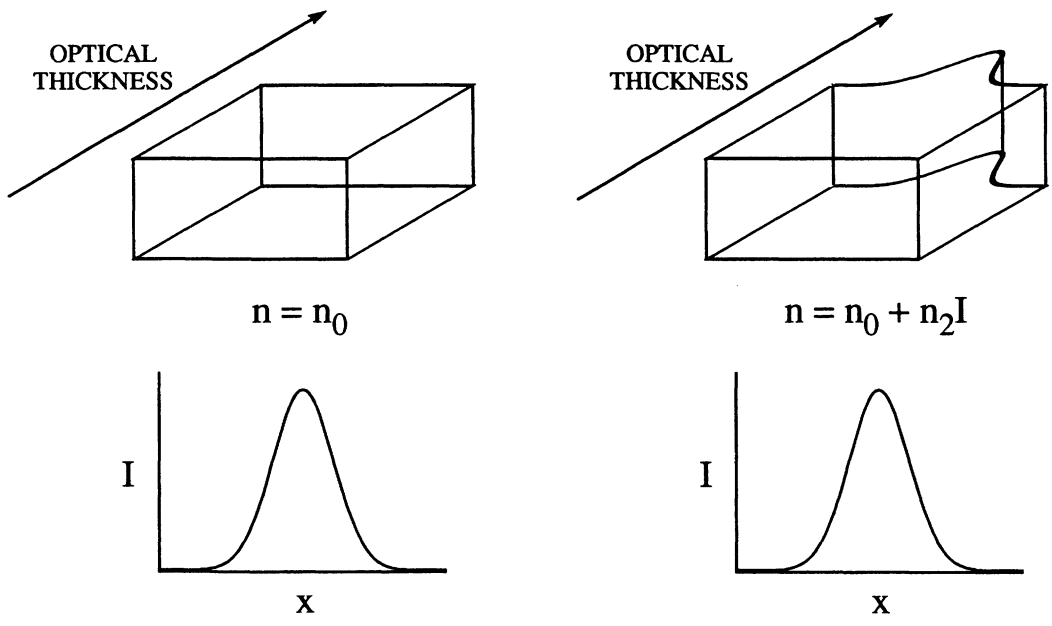

Figure 1. Simulation showing intensity dependent index.

While the Kerr limiter can be effective, it does suffer from two important difficulties. First, the laser intensity required before a significant value of $n_2 I$ can develop is extremely high and is generally on the order of megawatts per square centimeter (MW/cm^2). Since even milliwatts per square centimeter (mW/cm^2) continuous wave beams are dangerous to optical sensors, Kerr materials have restricted application. Second, once an index change $n_2 I$ is induced it affects all light passing through the material. This means that normal vision by the optical sensor does not

continue as long as laser light passes through it. These two restrictions make the Kerr limiter less than ideal.

PHOTOREFRACTIVE FOCUSING AND DEFOCUSING

In this paper, we present a new class of materials which produce dramatic focusing and defocusing effects[1]. These materials produce the same degree of focusing or defocusing independent of the incident intensity and produce an index change which only affects light of the same wavelength at propagation direction of the incident laser light. This class of materials, photorefractives, can potentially limit laser light of any intensity while maintaining normal vision through the material. Photorefractives would, therefore, appear to be a near optimal class of materials. There is, however, one difficulty with photorefractives. These materials have a much slower response than Kerr materials which are near instantaneous. Fortunately, this difficulty is not insurmountable. By simply reducing the incident laser light to a small spot at the material, sufficient intensities can be generated to produce the needed response time. For example, a typical response time for photorefractives is 0.1 s for an incident power of 1 W in a 1 centimeter diameter beam. If this beam is focused to a 100 μm spot the intensity in the material rises to 10^4 W/cm^2. Since the photorefractive response time is inversely proportional to the incident intensity this gives a response time of 10 μs. With a response time of 10 μs for an incident beam of 1 W in power, only 10 μJ are transmitted before focusing and defocusing are switched on. Since the photorefractive response time scales as the inverse of the intensity, 10 μJ is the amount of energy transmitted before focusing or defocusing is completed, independent of the incident power. That is, if P is the power of the incident beam and A its cross sectional area the energy transmitted through the limiters is

$$E = \int_0^\infty P_0 e^{-t/\tau} dt = C = \text{constant} \tag{2}$$

using $\tau = C/P_0$. For powers below 1 W the response time is longer than 10 μs, but the energy transfer per unit time is lower. The result is that 10 μJ is transmitted during the time that focusing or defocusing is developing. Likewise, for powers above 1 W the response time is faster than 10 μs, but the energy transfer per unit time is higher. As a result, 10 μJ is again the energy transmitted before focusing-defocusing is completed. In addition to reducing the incident spot size there are also other parameters which reduce the photorefractive response time. On the whole, therefore, photorefractives have the potential to act as the ideal defocusing or focusing device or corresponding optical limiter.

PHYSICAL MODEL

As in the case of Kerr focusing and defocusing, photorefractive focusing and defocusing can also be physically understood. To illustrate the photorefractive effect, we can first consider two plane waves of light overlapping in a crystal producing an optical interference pattern as shown in Figure 2. In the bright regions of the interference pattern carriers are excited into the conduction band. The excited carriers then diffuse or drift and are finally trapped in the dark regions of the interference pattern. The resulting charge separation in turn generates a space charge electric field. The drift and diffusion process continues until equilibrium is reached where the diffusion or drift current is exactly balanced by the current generated by the induced space charge field. In this way the magnitude of the field is simply determined by the value necessary to balance

the diffusion or drift current. The space charge field can then distort the lattice and produce via the electro-optic effect an index change given by

$$\Delta n = \frac{n^3}{2} r_{eff} E_{sc} \tag{3}$$

where r_{eff} is the effective electro-optic coefficient of the material, E_{sc} is the induced space charge field, and n is the unperturbed index of refraction of the material.

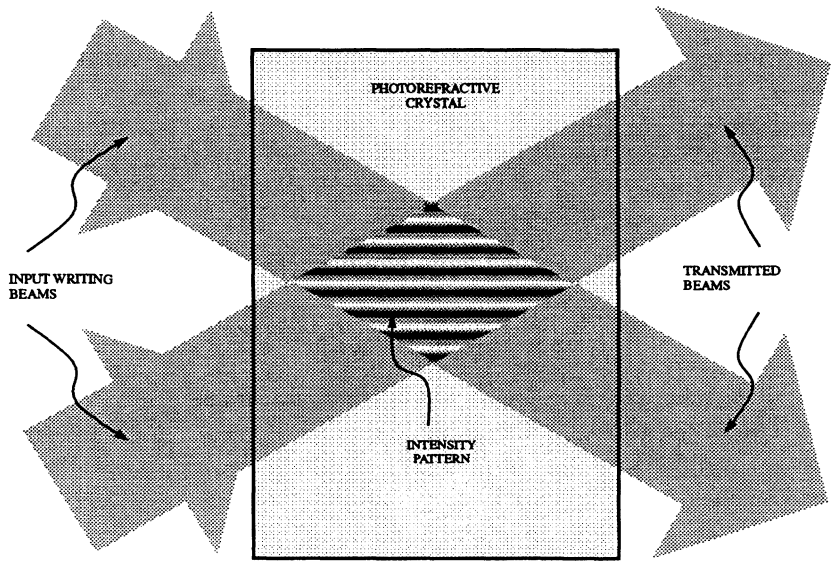

Figure 2. Illustration for the formation of photorefractive gratings.

The resulting induced index change can then be used in Maxwell's equation to predict the propagation behavior of the two overlapping laser beams. The result is that the induced index causes a coupling between the two beams which can be written as

$$\frac{dE_1}{dr_1} = i(\gamma_R + i\gamma_I)\frac{E_1|E_2|^2}{I_0} \tag{4a}$$

$$\frac{dE_2}{dr_2} = i(\gamma_R - i\gamma_I)\frac{E_2|E_1|^2}{I_0} \tag{4b}$$

where γ is the coupling coefficient and is determined by the material effective electro-optic coefficient and the magnitude of the laser-induced space charge field. The fact that γ has real and imaginary parts points out that the coupling between the two waves causes energy exchange between them and causes each of them to see a modified index of refraction.

In the physical picture we present here, we consider a propagating finite beam to be made up of Fourier plane-wave components. As shown in Figure 3(a) we can form a physical picture of diffraction that is based on "watching" each Fourier component propagating through the material. Since each component has a different k-vector projection along the propagation direction, the relative phase between Fourier components changes as a function of propagation distance z. Consequently, the sum of the Fourier components produces a different wave form at each z or propagation position. In the photorefractive picture each Fourier component produces an interference pattern with each and every other Fourier component. The result is that each component, therefore, "sees" a modified index of refraction which is determined by summing the index modification produced between a given Fourier component and every other component. When the low frequency Fourier components "see" a lower index than the higher frequency components due to the coupling, focusing is induced. (Fibure 3(b)) Likewise, when the low frequency components "see" a higher index than the higher frequency components, defocusing is induced (Figure 3(c)). In practice, the sign of the index change depends on the sign of an applied external field so that focusing is induced with an applied field along the c-axis direction while defocusing is produced with an applied field opposite the c-axis direction. One interesting possibility not discussed here occurs when diffraction is exactly compensated by photorefractive focusing. In this case, shape pursuing propagation or soliton formation is observed[2-5]. This picture neglects energy coupling which would result in an amplitude change of the Fourier components and would be important for a more complete analysis. In this paper the effect of energy coupling was minimized by the choice of input beam diameter, the value of applied field, and the time at which the measurement was made.

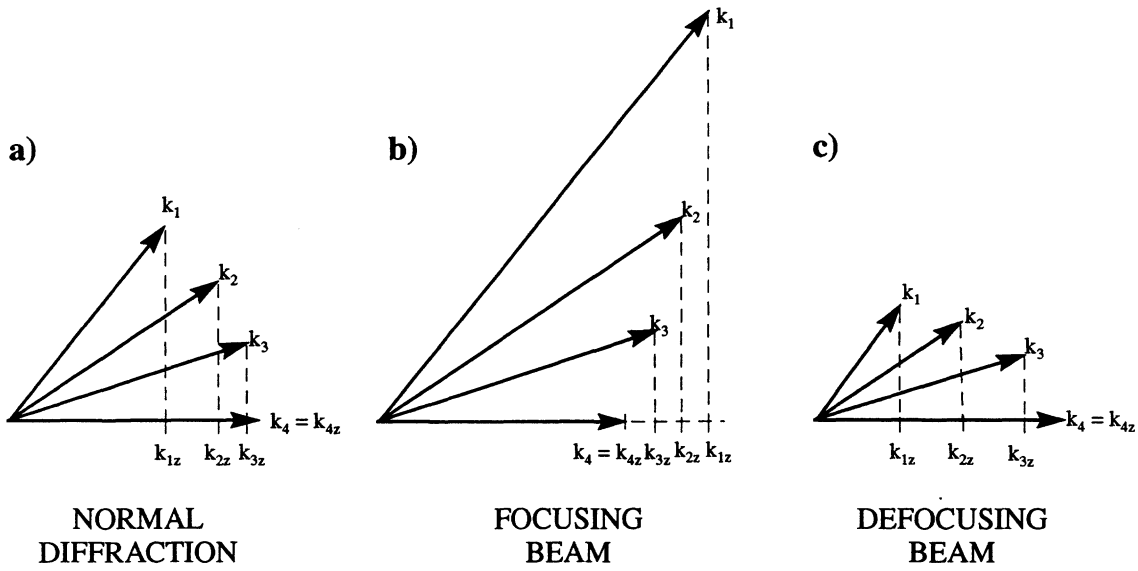

Figure 3. Wave-vector diagram of some of the Fourier components that make up a given laser spot showing what happens to the wave vectors as the beam passes through a photorefractive crystal with a) no voltage, b) an applied electric field parallel to the c-axis and c) an applied electric field anti-parallel to the c-axis.

EXPERIMENTAL OBSERVATIONS

The basic apparatus consisted of a cw argon-ion laser and a 5 mm x 5 mm x 6 mm strontium barium niobate (SBN) crystal with 0.01% by weight rhodium dopant. The cw argon-ion laser wavelength was 457 nm and its output beam diameter was 1.5 mm. A schematic diagram of the apparatus is shown in Figure 4. The output beam was directed onto a 10 cm focal length lens and the SBN crystal was placed 2.6 mm beyond the beam waist with $2\,w_0 = 33\ \mu m$. The beam diameter at the SBN crystal entrance face was 75 μm. The crystal was oriented with its c-axis in the horizontal plane and perpendicular to the propagation direction of the incoming laser light. The polarization of the incoming light could

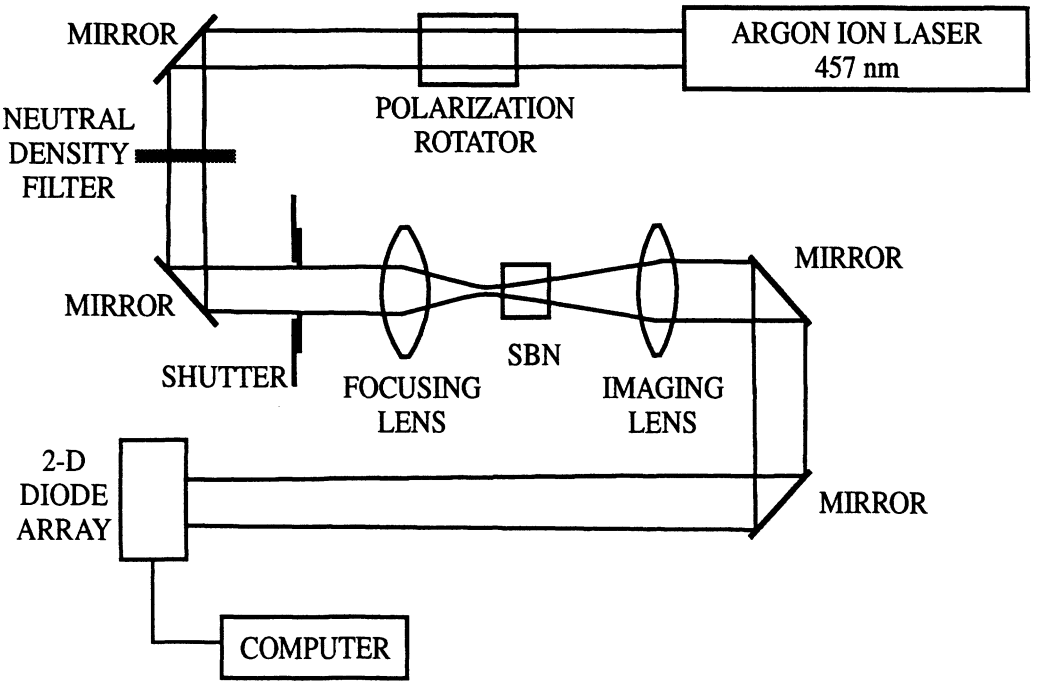

Figure 4. Experimental Apparatus

be varied using a polarization rotator but was initially chosen to be along the c-axis (extraordinary polarization). The beam diameter throughout the crystal was measured using an imaging system consisting of an imaging lens and a two-dimensional detector array. The input face of the 6 mm long SBN crystal was well beyond the Rayleigh range of 1.5 mm from the beam waist formed by

the focusing lens. The imaging system, therefore, imaged the beam spot at the SBN entrance face with some magnification onto the detector array. As the imaging lens and the detector array are moved away from the SBN crystal, different cross sections of the Gaussian beam are then imaged onto the array. In this manner, the beam diameter at different locations throughout the SBN crystal was monitored. The magnification of the imaging system was determined by placing a thin aperture on the crystal exit (and entrance) face and imaging the aperture onto the detector array. Using the known value of the reference aperture, the magnification was determined to be about 15.6 and the positions of the exit and entrance faces of the SBN crystal were located. Using this information the horizontal cross section of the incident beam on the entrance and exit faces of the crystal was determined. Beam diameter and viergence data where taken at a time when these quantities reached a maximum value.

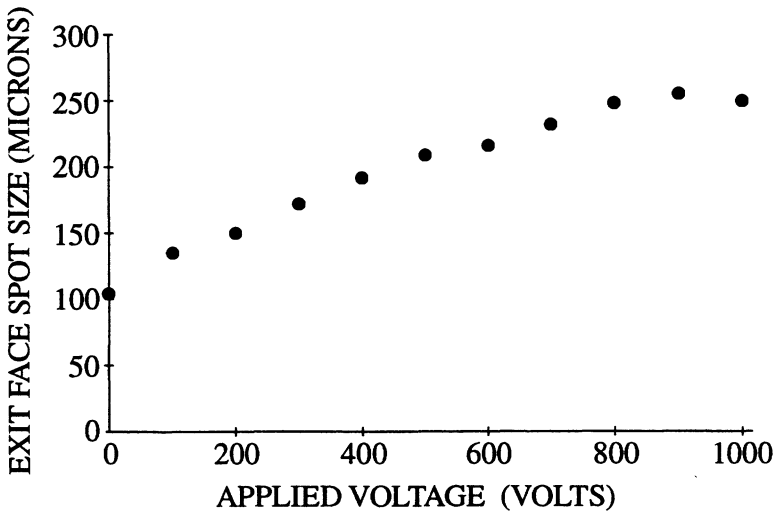

Figure 5. A graph showing the laser spot size diameter at the exit face of the crystal for different applied voltages.

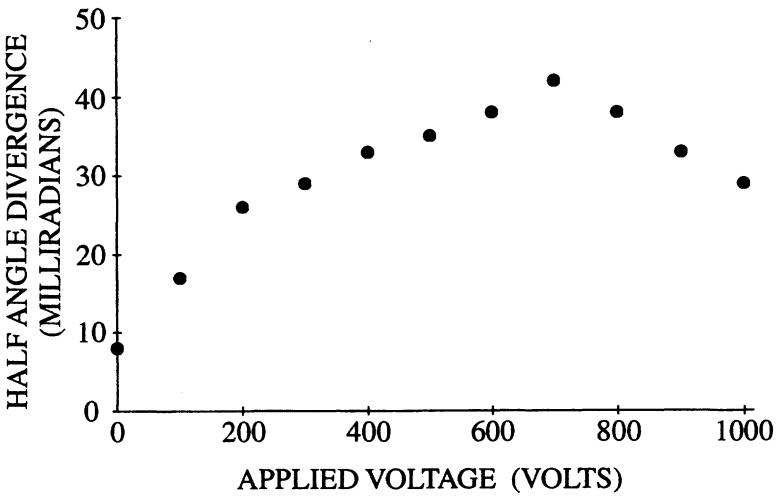

Figure 6. A graph showing the half angle divergence of the laser beam as it leaves the crystal with different applied voltages.

Figure 5 shows the effect of applied voltage on the exiting beam diameter while Figure 6 shows its effect on the divergence of the incident beam. As shown in these two figures the photorefractive defocusing is a dramatic effect. Similar results have been observed for focusing. Only the sign of the applied d.c. electric field was reversed when producing focusing or defocusing effects. Defocusing effects are seen when the field is opposite the c-axis direction.

CONCLUSION

In conclusion we have demonstrated that focusing and defocusing can be a dramatic effect in photorefractive crystals. This effect is also independent of the incident intensity, working at low intensities whereas the effects in Kerr matrerials are only present at high intensities. Both the focusing and defocusing effects were characterized for SBN:60 crystals. Similar results were found for all SBN samples as well as for BSKNN crystals. Photorefractive focusing and defocusing can now be investigated using traditional optical limiting geometries.

REFERENCES

1. M. Segev, Y. Ophir, and B. Fischer, Appl. Phys. Lett. **56**, 1086 (1990).

2. M. Segev, B. Crosignani, A. Yariv and B. Fischer, Phys. Rev. Lett. **68**, 923 (1992).

3. B. Crosignani, M. Segev, D. Engin, P. DiPorto, A. Yariv and G. Salamo, J. Opt. Soc. Am. **B 10**, 446 (1993).

4. G. Duree, J.L. Shultz, G. Salamo, M. Segev, A. Yariv, B. Crosignani, P. DiPorto, E. Sharp and R.R. Neurgaonkar, Phys. Rev. Lett. **71**, 533 (1993).

5. M. Segev, A. Yariv, G. Salamo, G. Duree, J. Shultz, B. Crosignani, P. DiPorto and E. Sharp, Opt. & Phot. News **4**, 8 (1993).